

Single-Carrier, Single- λ Full-Duplex Analog Radio Feed over a Single-Port RRH Transceiver

Bernhard Schrenk, *Member, IEEE*, and Fotini Karinou, *Member, IEEE*

Abstract—The densification of radio access and the massive deployment of radio heads calls for efficient optical fronthaul technologies. The adoption of analogue radio-over-fiber schemes promises greatly simplified equipment that can be distributed at the antenna sites for the purpose of radio signal conditioning and electro-optic conversion. Towards this direction, we propose and experimentally evaluate a full-duplex interface at the intersection between the optical and the radio frequency layer, aiming at bidirectional radio signal transmission over a single wavelength (1577 nm) and a single carrier frequency (5.375 GHz). Analogue coherent optical reception is performed through an electro-absorption modulated laser, which is employed as multi-functional element that accomplishes wavelength re-use for full-duplex radio-over-fiber transmission. The directional split is shifted to the electrical domain through adoption of a crosstalk-cancelling circulation stage, ensuring compatibility with a high dynamic power range for the simultaneous transmission and reception of up- and downlink radio signals, respectively, without the need for further duplexing methods subject to frequency translation or time slotting. We prove that margins of $>2\%$ in terms of error vector magnitude can be accomplished for an unpaired spectral configuration, where down- and uplink radio signals share the same spectrum in the optical and electrical domains.

Index Terms—Optical communication terminals, Optical signal detection, 5G mobile communication, Circulators

I. INTRODUCTION

HIGHER data rates, a higher user density and seamless coverage for next-generation radio access require a densification of the radio network. This is supported through a widespread deployment of remote radio heads (RRH), which shall be accompanied by a high degree of simplification of this field-distributed hardware at the antenna site [1]. In view of cloud-based radio networks with centralized baseband processing, as it is supported through antenna remoting by means of analogue radio-over-fiber transmission [2-5], this calls for improvements with respect to the opto-electronic RRH interface on the one hand, and transparent radio frequency (RF) electronics on the other hand. Up to now, most

optical fronthaul schemes rely on dedicated wavelengths to implement full-duplex transmission for down- and uplink radio signals, while at the same time analogue radio-over-fiber transmission has been primarily conducted using an intensity modulation / direct detection methodology. Both do not bode well with the spectral occupancy that can be obtained for a mobile optical fronthaul link. More importantly, it deviates from the typically filterless nature of brown-field fiber plants found in split-based passive optical access networks, since it requires a colored optical distribution network (ODN) that is typically based on dense wavelength division multiplexing (WDM) technology. This might impact the deployment opportunities at a later stage, such as the migration to wideband ODNs as currently foreseen for metro-core networks [6].

A second aspect of mobile fronthauling is the establishment of a transparent pipe from the air interface of the RRH to the centralized baseband unit (BBU). Implementations of an analogue fronthaul typically rely on a dual wavelength feed for simultaneous down- and uplink transmission over the optical fiber medium [7-11], meaning a pair optical spectrum for full-duplex radio signal transmission. Alternatively, wavelength re-use schemes can be adopted, as for example supported by means of orthogonal modulation [12]. With the use of a single wavelength to feed a RRH bidirectionally, it becomes difficult to retain an unpaired radio spectrum at the air interface, where the transmitted and received radio signals feature the same RF carrier frequency. This technical challenge owes to the sensitivity of weak radio signals to crosstalk arising from a simultaneously transmitted signal, whereas both signals are subject to a high dynamic range that covers ~ 7 orders of magnitude. In earlier works that focused on a single dual-function transceiver element for simultaneous signal transmission and reception, in-band crosstalk is avoided through the adoption of duplexing, which often requires to frequency-translate the radio signal before conversion to the optical domain is made [13, 14]. Alternatively, the bidirectional radio signals can be allocated to certain time slots before being transported over the optical layer [15], which nevertheless requires fast signal switching and end-to-end synchronization with the radio layer. In either case, the complexity at the RRH is increased for the sole purpose of establishing an optical fronthaul link. In order to achieve high cost efficiency for the field-deployed RRHs, it is therefore paramount to optically transport full-duplex radio signals over the same wavelength and at the same RF carrier frequency, in

Manuscript received May 31, 2022. This work was supported in part by the European Research Council (ERC) under the European Union's Horizon 2020 research and innovation programme (grant agreement No 804769).

B. Schrenk is with the AIT Austrian Institute of Technology, Center for Digital Safety&Security, Giefinggasse 4, 1210 Vienna, Austria (phone: +43 50550-4131; fax: -4150; e-mail: bernhard.schrenk@ait.ac.at).

F. Karinou is with Microsoft Research Ltd, Cambridge, CB1 2FB, United Kingdom (e-mail: fotini.karinou@microsoft.com).

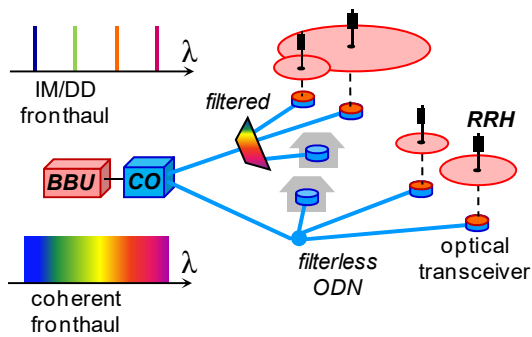


Fig. 1. Coherent mobile optical fronthaul with filterless ODN.

a manner that is maximally transparent to the radio layer.

This paper extends our initial analysis [16] on the full-duplex radio signal transmission over a simplified RRH interface supporting bidirectional analogue radio-over-fiber transmission over a single wavelength and single RF carrier frequency. The proposed coherent optical transceiver with single optical and single RF port leverages on a bleed-cancelling radio circulation stage in order to address the high dynamic range between received downlink and transmitted uplink signals with overlapping radio spectra. We will demonstrate that the single-wavelength / single-carrier concept can perform with $>2\%$ margins in terms of error vector magnitude (EVM) for 16/64-ary quadrature amplitude modulated (QAM) orthogonal frequency division multiplexed (OFDM) radio down-/uplink transmission.

The paper is organized as follows. Section II introduces the concept for the RRH interface with unpaired spectrum. Section III characterizes the directional branching device employed at the RF domain. Section IV discusses the experimental arrangement used for performance evaluation. The experimental performance of the proposed concept is discussed in Section V. Finally, Section VI concludes the work.

II. ANALOGUE MOBILE FRONTHAUL WITH SIMPLIFIED REMOTE RADIO HEAD

The introduction of a mobile optical fronthaul aims at a complexity reduction at the antenna sites by centralizing RF functions typically found at these remote sites [17]. For this sole reason of simplification of RRH equipment, this work shall further consider analogue radio-over-fiber transmission at the fronthaul link and, specifically, coherent analogue optical transmission. As introduced in Fig. 1, coherent technology enables a filterless ODN, a more spectrally efficient overlay, and a potentially higher optical budget.

A. Frequency-agnostic directional split at the RRH

The typical way to accomplish bidirectional, full-duplex radio signal transmission between the RRHs and BBUs is to dedicate separate wavelengths for the down- and uplink. Every RRH then features a receiver and transmitter, which in case of analogue radio-over-fiber transmission require linear electro-optic transfer characteristics. The directional split between down- and uplink, which are relayed over a shared fronthaul

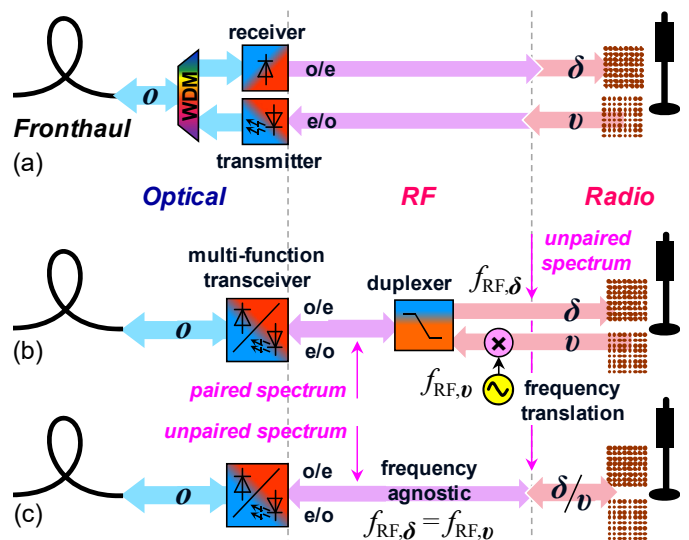


Fig. 2. RRH interfaces for full-duplex radio signal transmission exploiting (a) optical duplexing at the wavelength level, (b) RF duplexing at the frequency level using a paired radio spectrum, and (c) frequency-agnostic radio feed retaining an unpaired spectrum from the air to the optical interface.

feeder, can be accomplished in the optical domain through means of WDM. Such a deployment scenario is sketched in Fig. 2(a).

In an attempt to reduce the RRH complexity further, the directional split can be made in the RF domain. This greatly supports the reduction of cost since expensive optical functions are then off-loaded to RF circuitry. This flavor of full-duplex radio-over-fiber transmission over a single wavelength has been proposed and demonstrated earlier, featuring a single multi-function transceiver element [13-15]. However, shifting the directional split to the RF domain comes at the expense of additional frequency translation, as introduced in Fig. 2(b): Down- and uplink are typically sharing the same RF carrier frequency over the air interface, while the two signals then have to be separated through appropriate duplexing techniques in order to avoid crosstalk at the bidirectional mobile optical fronthaul. Frequency division duplexing (FDD) has been found as an attractive candidate to accomplish crosstalk suppression. It is further supported by the abundant bandwidth that opto-electronic systems offer. For example, 5G New Radio specifies radio signal bandwidths from 200 to 800 MHz [18], while commercial off-the-shelf opto-electronics offer bandwidths of more than 10 GHz. However, the translation of an unpaired radio spectrum at the air interface to a paired spectrum at the optical RRH interface requires means of frequency translation.

The conversion between paired and unpaired radio spectra breaks the transparency of the end-to-end radio link between the mobile user and the BBU. This work therefore aims to remove this frequency translation while retaining an unpaired spectral configuration over the end-to-end radio link, covering RF and optical layers. With this, the optical RRH interface does not perturb the original spectral layout of the radio signal when passing it from the air over the fiber-based mobile fronthaul to a centralized radio processing unit. In order to accomplish this target through a “colorless” or frequency-

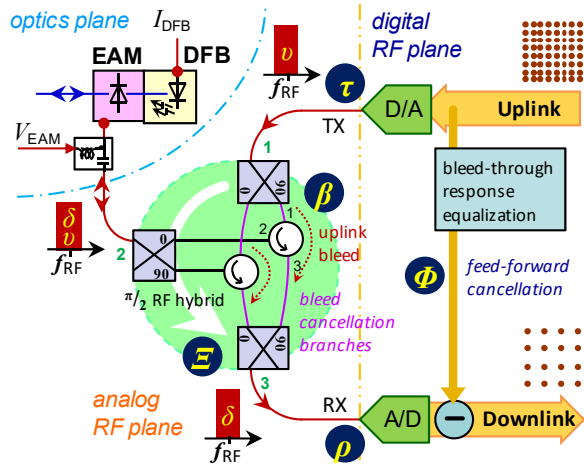


Fig. 3. Opto-electronic RRH interface for bidirectional down-/uplink radio signal transmission.

agnostic directional split (Fig. 2(c)), the overlapping radio signal spectra for down- and uplink require a good separation, especially due to the high dynamic range in RF power that is associated to the down- and uplink signals launched towards the air interface and the fronthaul. In this work, we will focus on the RRH interface, where a weak downlink signal is received from the central office, while a strong uplink is delivered by the RRH at the same time. As such, we will demonstrate full-duplex analogue radio-over-fiber transmission in continuous mode over a single wavelength and a single RF carrier frequency, utilizing a simplified opto-electronic transceiver with a single optical and RF port.

B. Coherent analogue fronthaul for filterless ODN

In order to achieve bidirectional transmission over a single RRH transceiver with single optical and single RF port, a dual-function element is required. This device has to accommodate the electro-optic functions of photodetection and optical transmission. In this work, we will build on an electro-absorption modulator to serve this purpose. The versatile use of an EAM has been proposed earlier [19-21] and investigated for various applications [22]. In principle, an optically amplified and locally fed EAM could be used for signal detection and signal modulation, respectively, provided that optical filtering is adopted at the ODN.

The present work builds on our earlier scheme, which exclusively demonstrated analogue coherent detection of a downlink signal [23] and embeds this dual-function EAM element in a coherent transceiver arrangement. The adoption of coherent detection at the RRH greatly simplifies the fiber plant towards a filterless ODN (Fig. 1) by virtue of the signal selection function inherent to the coherent RRH receiver.

Specifically, an electro-absorption modulated laser (EML) comprising of a distributed feedback (DFB) laser and an EAM is applied as (single-polarization) multi-functional coherent transceiver element in Fig. 2(c). The incident radio signal beats with the local oscillator emission of the DFB laser at the EAM photodiode, thus accomplishing coherent detection. With the EAM biased at partial transparency, a portion of the radio signal passes to the DFB laser. In case of a small

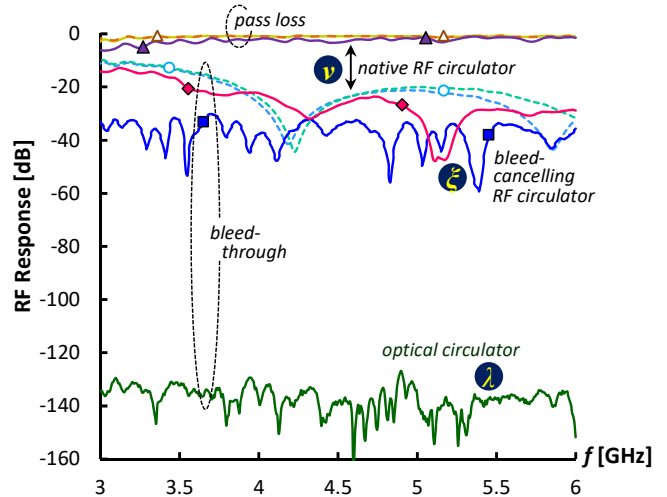


Fig. 4. Response of standard RF circulators and the bleed-cancelling RF circulator employed as directional split at the RRH interface.

detuning, the DFB emission is injection-locked to the radio signal, leading to optical frequency synchronization [24] and, consequently, homodyne detection. As reported in [25], stable locking of the DFB emission can be achieved for low optical power levels of -30 dBm injected to the EML, provided that both involved optical sources are temperature-stabilized.

At the same time, the EAM bias at partial transparency is compatible with electro-optical modulation through the same EAM. This allows for simultaneous uplink transmission, provided that a directional split can be facilitated in the RF domain. Our recent work [14, 25] exploited FDD for this purpose, at the expense of additional frequency translation for one of the radio signals, as discussed earlier (Fig. 2(b)).

III. DIRECTIONAL SPLIT FOR UNPAIRED RADIO SPECTRUM

A directional split in the RF domain could be in principle accomplished through the use of a RF circulator at the bidirectional transmit/receive port of the full-duplex opto-electronic transceiver, which in case of the proposed coherent homodyne EML transceiver relates to the electrical port of the EAM. However, unlike an optical circulator, the RF counterpart is subject to a strong bleed-through between its ports 1 and 3, where no signal transfer is intended. A re-design of the circulating stage at the RF domain is therefore required. Figure 3 introduces the proposed directional split method. It aims to minimize the bleed-through (β) of the strong uplink radio signal, to be transmitted by the EML, towards the much weaker downlink radio received by the EML.

A typical bleed-through characteristic of a RF circulator is reported in Fig. 4. It shows the native isolation (v) between ports 1 and 3 of two RF circulator devices. The isolation features rather low values over its operating bandwidth from 4 to 8 GHz and has a peaking maximum of only 43.9 dB caused by a resonant behavior (\circ). Figure 4 further compares the port 1-3 isolation to that of an optical circulator (λ), which features an orders-of-magnitude higher value of more than 127 dB in the RF domain.

The circulating stage \mathcal{E} that constitutes the directional split

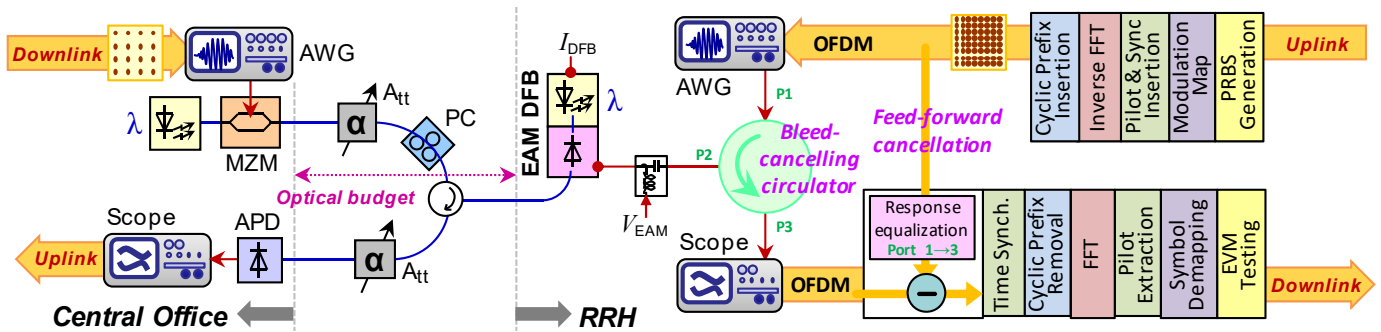


Fig. 5. Experimental setup to evaluate a coherent optical RRH interface for bidirectional, full-duplex radio signal transmission with unpaired spectrum.

has been therefore modified in order to address the insufficient crosstalk suppression of the uplink signal at port 1. A bleed-cancelling circuit has been included by branching the entire circulating stage through 90° RF hybrids before adopting RF circulators. Given the port-specific phase setting of the hybrids in Fig. 3, the resulting branches between the three ports of the overall circulating stage \mathcal{E} combine constructively between the RF transmit port τ to the EAM and from the EAM to the receiver, corresponding to the known transparent setting between ports 1-2 and ports 2-3 of a circulator. Moreover, the branches combine destructively between the RF transmit port τ and the reception port ρ , corresponding to a port 1-3 setting. This mitigates bleed-through of the native RF circulators employed within the two branches, as they have been characterized earlier. The extinction and bandwidth for the bleed suppression clearly depends on the performance of the involved RF hybrids and the sandwiched circulators, and the capability of wideband matching for the two branches. In the present experiment, we relied on discrete components to implement the bleed-cancelling circulating stage \mathcal{E} , whereas monolithic microwave integrated circuits would be clearly the preferable option.

Figure 4 includes the performance of two different implementations for the bleed-cancelling circulating stage. These involve two different sets of 90° RF hybrids for operation from 2 to 8 GHz with an amplitude / phase imbalance of 0.4 dB / 5 degrees (set 1) and 0.5 dB / 2 degrees (set 2) over this spectral region, and the RF circulators rated for an isolation of >20 dB from 4 to 8 GHz. Compared to the native isolation ν of the RF circulators, the isolation ($\blacklozenge, \blacksquare$) between ports τ and ρ of the bleed-cancelling circulating stage is improved over the entire spectrum. It features a maximum of isolation that is enhanced by more than 15 dB (\blacksquare). As indicated before, the resulting ripple in the response between ports τ and ρ and the limited suppression bandwidth of the isolation maximum (ζ) of ~ 120 MHz (\blacklozenge), which at this point is not enough to address 5G New Radio bandwidth requirements, is explained by the limited ability to precisely balance both cancellation branches in phase and, more important, loss over a wideband frequency range when employing discrete RF components. We therefore chose to optimize this balance between the two branches for a high RF carrier frequency in the sub-6GHz range. Despite the inclusion of additional components at the circulating stage, the insertion

loss between the EAM and RF receiver (ρ) ports remains acceptably low with 1.5 dB (\blacktriangle) at 5.4 GHz. A similar value was found between the RF transmitter (τ) and EAM ports.

It shall be stressed that the accomplished isolation of up to 59 dB does not only contribute to the analogue crosstalk suppression of uplink bleed-through at the reception port (ρ). It further levels the received signal at this port in a manner that its magnitude, which is jointly determined by the optically received downlink and the uplink RF crosstalk noise, is not primarily defined by the uplink crosstalk anymore. In this new regime, where the signal-to-noise ratio (SNR) is >1 for the received downlink, as we will prove later, the compound received signal now adheres more favorable to the dynamic range of the analogue-to-digital converter (ADC) of a subsequent radio receiver. This is because the effective number of bits can be significantly increased for the downlink signal, rather than a stronger in-band uplink noise limiting the acquisition capability for a weaker downlink signal with a $\text{SNR} \ll 1$. Under this condition, further in-band uplink noise mitigation is thinkable using a simple digital feed-forward cancellation, as indicated in Fig. 3 (Φ). The present experiment will employ such a cancellation circuit to additionally boost the SNR.

It shall be further stressed that in a practical RRH implementation, the uplink RF signal will be subject to signal fading during RF free-space propagation. This results in a large dynamic RF power range, which would necessitate a RF signal amplification stage that delivers a compatible drive level for the optical uplink modulator at all times, for example by involving a programmable gain amplifier.

IV. EXPERIMENTAL SETUP

Figure 5 presents the experimental setup to evaluate the bidirectional RRH interface for full-duplex coherent analogue radio-over-fiber transmission with unpaired spectral configuration.

The downlink radio was generated as OFDM signal at a RF carrier frequency of $f_{\text{RF}} = 5.375$ GHz through an arbitrary waveform generator (AWG). The OFDM signal had 128 sub-carriers and a bandwidth of 62.5 MHz. This signal bandwidth was aligned with the accomplished peak-isolation bandwidth of the bleed-cancelling circulator, as reported in Section III. The radio signal was modulated on an optical carrier at $\lambda = 1577$ nm using a Mach-Zehnder modulator (MZM).

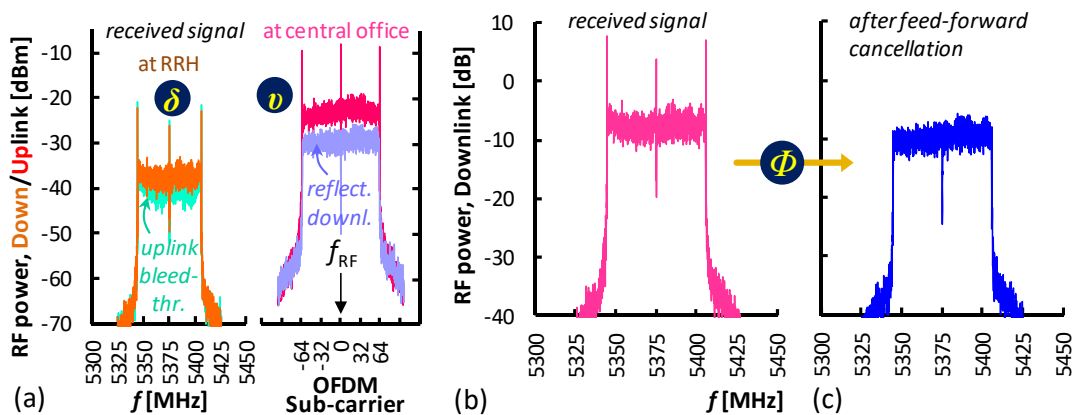


Fig. 6. (a) Received down- (δ) and uplink (ν) spectra after photodetection. Received downlink signal before (b) and after (c) uplink cancellation.

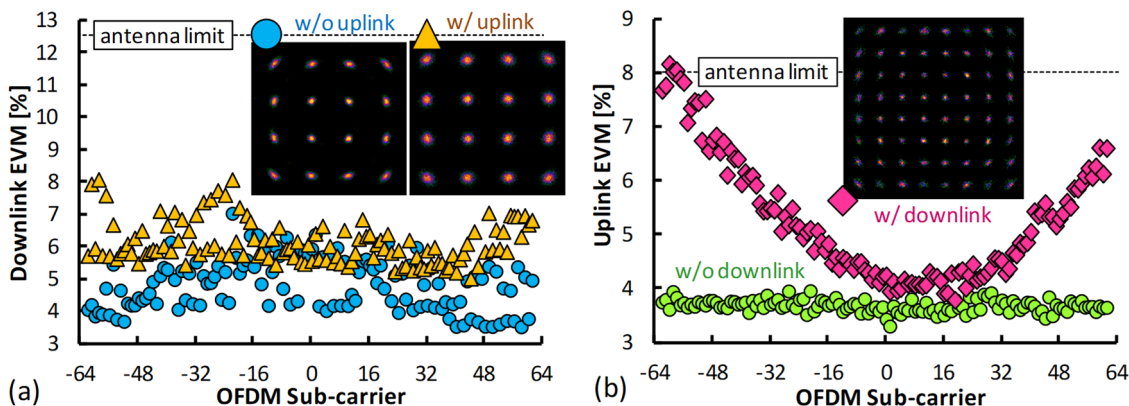


Fig. 7. EVM per subcarrier for full- and half-duplex (a) downlink and (b) uplink radio signal transmission.

The downlink was injected to the EML at the RRH at a power level of -12 dBm after passing an optical loss budget of 15 dB between MZM and EML. No fiber-based ODN has been used for this evaluation to rule out additional penalties that would overcast those associated to the proposed full-duplex RRH interface. However, the treatment of fiber impairments specific to the proposed reflective coherent receiver architecture can be found elsewhere [26]. It shall also be noted that a single-polarization design of the EML receiver has been employed for the sake of simplicity, accompanied by a manual polarization controller (PC) that accounts for state-of-polarization alignment. However, the polarization-independent operation of the EML-based receiver has been demonstrated earlier [27].

The transistor-outline EML was temperature-stabilized through a micro-Peltier element. With this, stable injection-locking can be guaranteed and the DFB emission is frequency-synchronized to the optical carrier of the downlink, while a stable phase between the DFB-based local oscillator emission and the incident radio signal is accomplished at the same time [23]. The EAM was biased at -0.7V, which sets its operation point as multi-function element that simultaneously acts as semi-transparent modulator and photodiode.

At the RRH, an uplink radio signal is generated at the same RF carrier frequency f_{RF} and fed to the RF transmit port of the RRH interface. The uplink OFDM signal features the same signal bandwidth and the same number of sub-carriers as the

downlink, in view of an unpaired spectral configuration. However, the down- and uplink OFDM radio signals were decorrelated with respect to the modulation format: While 16-QAM has been used for the downlink, the sub-carriers of the uplink signal were modulated with 64-QAM. The uplink drive for converting the radio signal from the RF to the optical domain through the dual-function EML was variably adjusted in order to investigate the trade-off in terms of residual crosstalk for the simultaneously received downlink radio signal. An optical circulator separates the down- and uplink signals in order to relay the uplink to an avalanche photodiode (APD) based receiver at the central office. According to the optical budget in downlink direction, a symmetric 15-dB budget has been set for uplink reception.

The evaluation of the down- and uplink radio signals received at the RRH and the central office have been conducted in terms of EVM estimations. For this purpose, the signals have been digitized by a real-time scope. The feed-forward cancellation, which has been included in the evaluation, builds on the previously acquired frequency response of the RF circuit to spectrally shape the forward uplink cancellation signal. This involves channel sounding over the analogue RF circulating stage \mathcal{E} between the interfaces of the digital-to-analogue converter (DAC) and the ADC, and pilot information that has been included on three of the OFDM sub-carriers in either radio signal to further serve the adjustment of the cancellation magnitude. The power

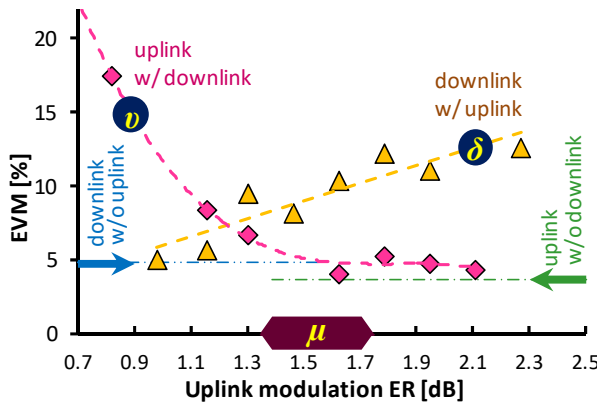


Fig. 8. Down-/uplink EVM dependence on the uplink modulation ER.

allocated to these pilot tones was the same as for a data sub-

V. RESULTS AND DISCUSSION

A. Received radio signal spectra

Figure 6(a) presents typical RF spectra for the received down- and uplink signals. The spectra have been directly acquired after photodetection. Thanks to coherent homodyne reception, the downlink OFDM spectrum (δ) is clearly delimited and does not feature a frequency offset with respect to the original RF carrier frequency f_{RF} . The uplink bleed-through at the received RRH, included in Fig. 6(a), has been recorded under absence of a downlink signal and indicates the magnitude of crosstalk overlapping at the downlink branch.

It is noteworthy to stress that the uplink (ν) spectrum that is received at the central office is also showing a crosstalk component. This component results from the reflective nature of the coherent EML transceiver at the RRH, which causes a partial reflection of the downlink into the uplink direction. This crosstalk note necessitates a similar feed-forward cancellation for the uplink reception, though it is in principle not seen as a practical approach due to its nature as a time-delayed far-end crosstalk. Its mitigation would rather require a re-design of the RRH transceiver, which is left for future work.

Figure 6(b) reports a characteristic downlink spectrum before and after feed-forward cancellation, for a highest uplink intensity modulation extinction ratio (ER) of 2.1 dB used in this work. The pilot tones embedded with the uplink signal discipline the cancellation (Φ in Fig. 3), which aims to remove the residual uplink crosstalk over the entire downlink spectrum through RF phase and magnitude adjustment. The recovered downlink signal, originally transmitted as a pilot-free signal and shown in Fig. 6(c) after its reception, does therefore not feature these pilot tones anymore.

B. Radio signal transmission performance

Figure 7 presents the full-duplex EVM performance per subcarrier for the downlink (δ , \blacktriangle) and uplink (ν , \blacklozenge) radio signal with an uplink ER of 1.8 dB. Comparison is made with half-duplex transmission (\bullet) for either signal direction. An average downlink EVM of 6.1% has been achieved (\blacktriangle). This

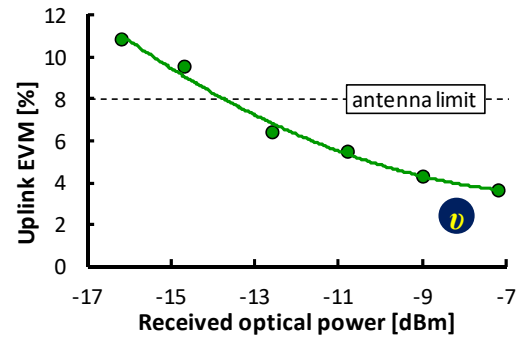


Fig. 9. Uplink EVM as function of the received optical power.

is slightly above the EVM of 4.8% obtained for half-duplex transmission. The low EVM penalty evidences the efficiency of the frequency-agnostic directional split in the RF domain. For the uplink direction, average EVM values of 5.3% (\blacklozenge) and 3.7% (\bullet) are obtained. The EVM increase towards lower and upper OFDM sub-carriers present for the full-duplex uplink EVM (\blacklozenge) is believed to originate from a sub-optimal and time-variant far-end downlink crosstalk noise cancellation employed at the central office over both, electrical and optical domains. In all cases, clear constellation diagrams have been obtained and the average EVM values are clearly below the EVM antenna limits for 16- and 64-QAM radio signal transmission.

The EVM dependence for both radio signal transmission directions on the uplink ER is reported in Fig. 8, with the half-duplex performance being indicated through arrows.

The downlink EVM (\blacktriangle) increases steadily with the uplink magnitude. It remains within the antenna limit of 12.5% for 16-QAM OFDM transmission, which is surpassed for an uplink ER of 2.1 dB. Even though this ER appears to be low at first glance, it is close to the typical 3-dB value which is often adopted in wavelength re-use schemes applied in full-duplex wired optical access networks [28]. This ER value is also sufficiently high to support 64-QAM OFDM uplink transmission at a very low EVM of 4.4% (\blacklozenge), which leaves ample margin to the corresponding EVM antenna limit of 8%. For this reason, the uplink ER can be further reduced to improve the downlink EVM, down to an ER value of 1.15 dB. Aiming at a balanced EVM margin of $>2\%$ for both radio signal transmission directions, an upstream ER range between 1.34 and 1.75 dB is preferred for the given setup (μ in Fig. 8).

Figure 9 shows the uplink EVM performance at a low $\mu = 1.3$ dB within the aforementioned ER range, as function of the received optical power at the APD receiver of the central office. Results are reported for half-duplex uplink transmission. Values below the EVM antenna limit can be obtained, down to a received optical power of -13.8 dBm. This rather limited reception sensitivity is attributed to the penalty associated to the reduced intensity modulation ER of the uplink signal [29].

A further reduction in received downlink signal power, which had been presently set to -12 dBm, while retaining low EVM values for signal reception at the same time, would require an improvement in crosstalk suppression by the bleed-

cancelling circulator. This can be accomplished through a more integrated and thus matched RF design for the constituent branches of this directional split device. It would further permit an increase in uplink ER, thus alleviating the uplink reception from its current penalty inherent to its strongly reduced intensity modulation index.

Moreover, we see improvement potential in terms of downlink sensitivity and supported radio signal bandwidth and/or modulation efficiency through an inclusion of a transimpedance-amplifier based receiving front-end, which would have to be co-integrated with the circulation stage.

VI. CONCLUSION

We have experimentally demonstrated a full-duplex RRH transceiver realizing bidirectional radio signal transmission over a single wavelength and a single RF carrier frequency, thus implementing a truly transparent end-to-end connection between the air interface and centralized baseband processing. We introduced a concerted approach for analogue coherent optical reception in filterless ODNs and directional signal branching in the RF domain, accomplished through a crosstalk-mitigating circulator. The proposed RRH interface built on a single-port, multi-function modulator/detector device at the optical layer, implemented through an EML. In order to expand the resource-efficient use of spectral assets to the RF domain, a bleed-cancelling circulator has been adopted as directional splitting stage, ensuring that crosstalk between the strong uplink radio signal at the RRH towards the weak downlink signal received over the optical fronthaul link is minimized. Together with additional feed-forward cancellation, which is operated in a regime where the received radio signal features the same order of magnitude as in-band crosstalk, EVM margins beyond 2% have been achieved for full-duplex 16-QAM / 64-QAM OFDM down/uplink radio transmission at the same sub-6GHz RF carrier frequency. Wideband operation of the employed bleed-cancelling circulator and improved crosstalk mitigation are expected for a higher degree of RF circuit integration, which would allow a better balancing of RF paths within the directional splitting stage. Millimeter-wave operation is also left for future work.

REFERENCES

- [1] I. A. Alimi, A. L. Teixeira and P. P. Monteiro, "Toward an Efficient C-RAN Optical Fronthaul for the Future Networks: A Tutorial on Technologies, Requirements, Challenges, and Solutions", *IEEE Comm. Surveys & Tutorials*, vol. 20, no. 1, pp. 708-769, Firstquarter 2018.
- [2] M. Sung *et al.*, "RoF-based radio access network for 5G mobile communication systems in 28 GHz millimeter-wave," *IEEE/OSA J. Lightwave Technol.*, vol. 38, no. 2, pp. 409-420, Jan. 2020.
- [3] K. Kanta *et al.*, "Analog fiber-wireless downlink transmission of IFoF/mmWave over in-field deployed legacy PON infrastructure for 5G fronthauling," *IEEE/OSA J. Opt. Comm. Netw.*, vol. 12, no. 10, pp. 57-65, Oct. 2020.
- [4] S. Ishimura, A. Bekkali, K. Tanaka, K. Nishimura, and M. Suzuki, "1.032-Tb/s CPRI-equivalent rate IF-over-fiber transmission using a parallel IM/PM transmitter for high-capacity mobile fronthaul links," *IEEE/OSA J. Lightwave Technol.*, vol. 36, no. 8, pp. 1478-1484, Apr. 2018.
- [5] H.N. Parajuli, H. Shams, L. Guerrero Gonzalez, E. Udvary, C. Renaud, and J. Mitchell, "Experimental demonstration of multi-Gbps multi sub-bands FBMC transmission in mm-wave radio over a fiber system," *OSA Opt. Expr.*, vol. 26, no. 6, pp.7306-7312, Mar. 2018.
- [6] A. Nespolo *et al.*, "Transmission of 61 C-Band Channels Over Record Distance of Hollow-Core-Fiber With L-Band Interferers," *IEEE/OSA J. Lightwave Technol.*, vol. 39, no. 3, pp. 813-820, Feb. 2021.
- [7] D.N. Nguyen *et al.*, "Full-duplex transmission of multi-Gb/s subcarrier multiplexing and 5G NR signals in 39 GHz band over fiber and space," *Appl. Opt.*, vol. 61, no. 5, pp. 1183-1193, Feb. 2022.
- [8] J. Kim *et al.*, "MIMO-Supporting Radio-Over-Fiber System and its Application in mmWave-Based Indoor 5G Mobile Network," *IEEE/OSA J. Lightwave Technol.*, vol. 38, no. 1, pp. 101-111, Jan. 2020.
- [9] L. Bogaert *et al.*, "SiPhotonics/GaAs 28-GHz Transceiver With Reflective EAM for Laser-Less mmWave-Over-Fiber," *IEEE/OSA J. Lightwave Technol.*, vol. 39, no. 3, pp. 779-786, Feb. 2021.
- [10] Z. Tang, J. Zhang, S. Pan, G. Roelkens, and D. Van Thourhout, "Ring-modulator-based RoF system with local SSB modulation and remote carrier reuse," *Electron. Lett.*, vol. 55, no. 20, pp. 1101-1104, Oct. 2019.
- [11] J. Pérez Santacruz, G. Nazarikov, S. Rommel, A. Jurado-Navas, and I. Tafur Monroy, "Bidirectional ARoF fronthaul over multicore fiber for beyond 5G mm-wave communications," *Opt. Communications*, vol. 521, p. 128591, 2022.
- [12] B. Wenlin *et al.*, "A WDM-PON compatible wavelength-reused bidirectional in-band full-duplex radio-over-fiber system," *Opt. Communications*, vol. 463, p. 125408, 2020.
- [13] A. Stöhr, K. Kitayama, and D. Jäger, "Full-Duplex Fibre-Optic RF Subcarrier Transmission Using a Dual-Function Modulator/Photodetector," *IEEE Trans. Microw. Theory and Tech.*, vol. 47, no. 7, pp. 1338-1341, Jul. 1999.
- [14] B. Schrenk, "The EML as Analogue Radio-over-Fiber Transceiver – a Coherent Homodyne Approach," *IEEE/OSA J. Lightwave Technol.*, vol. 37, no. 12, pp. 2866-2872, Jun. 2019.
- [15] M.P. Thakur *et al.*, "480-Mbps, Bi-Directional, Ultra-Wideband Radio-Over-Fibre Transmission Using a 1308/1564-nm Reflective Electro-Absorption Transducer and Commercially Available VCSELs," *IEEE/OSA J. Lightwave Technol.*, vol. 27, no. 3, pp. 266-272, Feb. 2009.
- [16] B. Schrenk, and F. Karinou, "First Demonstration of a Single- λ , Full-Duplex RRH Transceiver with Single RF Carrier for Bidirectional Radio", in *Proc. Opt. Fib. Comm. Conf. (OFC)*, San Diego, United States, Mar. 2022, paper W4C.1.
- [17] M. Peng, Y. Sun, X. Li, Z. Mao, and C. Wang, "Recent Advances in Cloud Radio Access Networks: System Architectures, Key Techniques, and Open Issues," *IEEE Comm. Surveys & Tutorials*, vol. 18, no. 3, pp. 2282-2308, Thirdquarter 2016.
- [18] S. Parkvall, E. Dahlman, A. Furuskär, and M. Frenne, "NR: The New 5G Radio Access Technology," *IEEE Comm. Standard Mag.*, vol. 1, no. 4, pp. 24-30, Dec. 2017.
- [19] Q. Nguyen *et al.*, "Multi-Functional R-EAM-SOA for 10-Gb/s WDM Access," in *Proc. Opt. Fib. Comm. Conf. (OFC)*, Los Angeles, USA, Mar. 2011, paper OThG7.
- [20] R. Welstand, S. Pappert, C. Sun, J. Zhu, Y. Liu, and P. Yu, "Dual-Function Electroabsorption Waveguide Modulator/Detector for Optoelectronic Transceiver Applications," *IEEE Phot. Technol. Lett.*, vol. 8, no. 11, pp. 1540-1542, Nov. 1996.
- [21] A. Garreau *et al.*, "10 Gbit/s Drop and Continue Colorless Operation of a 1.5 μ m AlGaInAs Reflective Amplified Electroabsorption Modulator," in *Proc. Europ. Conf. Opt. Comm. (ECOC)*, Cannes, France, Sep. 2006, We.1.6.5.
- [22] B. Schrenk, "The Electroabsorption-Modulated Laser as Optical Transmitter and Receiver: Status and Opportunities", *IET Optoelect.*, vol. 14, no. 6, pp. 374-385, Dec. 2020.
- [23] B. Schrenk, M. Hofer, and T. Zemen, "Analogue Receiver for Coherent Optical Analogue Radio-over-Fiber Transmission," *OSA Opt. Lett.*, vol. 42, no. 16, pp. 3165-3168, Aug. 2017.
- [24] R. Hui, A. D'Ottavi, A. Mecozzi, and P. Spano, "Injection Locking in Distributed Feedback Semiconductor Lasers," *IEEE J. Quantum Elect.* vol. 27, no. 6, pp. 1688-1695, Jun. 1991.
- [25] B. Schrenk, and F. Karinou, "A Coherent Homodyne TO-Can Transceiver as Simple as an EML," *IEEE/OSA J. Lightwave Technol.*, vol. 37, no. 2, pp. 555-561, Jan. 2019.
- [26] B. Schrenk, N. Vokic, D. Milovancev, and F. Karinou, "Full-Duplex, Polarisation-Independent Coherent Homodyne EML Transceiver", in *Proc. Europ. Conf. Opt. Comm. (ECOC)*, Dublin, Ireland, Sep. 2019, paper Tu.3.D.6.

- [27] B. Schrenk, and F. Karinou, "Simple Laser Transmitter Pair as Polarization-Independent Coherent Homodyne Detector," *OSA Opt. Expr.*, vol. 27, no. 10, pp. 13942-13950, May 2019.
- [28] B. Schrenk, F. Bonada, M. Omella, J.A. Lazaro, and J. Prat, "Enhanced Transmission in Long Reach WDM/TDM Passive Optical Networks by Means of Multiple Downstream Cancellation Techniques," in *Proc. Europ. Conf. Opt. Comm. (ECOC)*, Vienna, Austria, Sept. 2009, paper We.8.5.4.
- [29] H. Takesue, N. Yoshimoto, Y. Shibata, T. Ito, Y. Tohmori, and T. Sugie, "Wavelength Channel Data Rewriter Using Semiconductor Optical Saturator/Modulator," *IEEE/OSA J. Lightwave Technol.*, vol. 24, no. 6, pp. 2347-2354, Jun. 2006.

Bernhard Schrenk (S'10-M'11) was born 1982 in Austria and received the M.Sc. ('07) degree in microelectronics from the Technical University of Vienna. He was at the Institute of Experimental Physics of Nobel laureate Prof. A. Zeilinger, where he was involved in the realization of a first commercial prototype for a quantum cryptography system, within the European SECOQC project. From 2007 to early 2011 he obtained his Ph.D degree at UPC BarcelonaTech, Spain. His Ph.D thesis on multi-functional optical network units for next-generation Fiber-to-the-Home access networks was carried out within the FP7 SARDANA and EURO-FOS projects. In 2011 he joined the Photonic Communications Research Laboratory at NTUA, Athens, as post-doctoral researcher and established his research activities on coherent FTTH under the umbrella of the FP7 GALACTICO project. In 2013 he established his own research force on photonic communications at AIT Austrian Institute of Technology, Vienna, where he is working towards next-generation metro-access-5G networks, photonics integration technologies and quantum optics.

Dr. Schrenk has authored and co-authored ~200 publications in top-of-the-line (IEEE, OSA) journals and presentations in the most prestigious and highly competitive optical fiber technology conferences. He was further awarded with the Photonics21 Student Innovation Award and the Euro-Fos Student Research Award for his PhD thesis, honoring not only his R&D work but also its relevance for the photonics industry. He is serving as Technical Program Committee member for the ECOC and OFC conferences. During his extensive research activities he was and is still engaged in several European projects such as SARDANA, BONE, BOOM, APACHE, GALACTICO, EURO-FOS and the Quantum Flagship project UNIQORN. In 2013 he received the European Marie-Curie Integration Grant WARP-5. In 2018 he was awarded by the European Research Council with the ERC Starting Grant COYOTE, which envisions coherent optics everywhere.

Fotini Karinou (S'09-M'13) was born in Arta, Greece, in 1983. She received the Diploma in Electrical and Computer Engineering, with specialization in telecommunications and information theory, and the PhD degree in optical communications focused on spectrally efficient WDM optical interconnect networks with advanced modulation formats, from the University of Patras, Greece, in 2007, and 2012, respectively. In 2007, she was a visiting researcher in the Institute for Quantum Optics and Quantum Information (IQOQI), at Vienna University of Technology, participating in the initial attempts for the realization of a commercial prototype of a quantum key distribution system based on polarization entanglement in the Institute of Experimental Physics of Prof. Zeilinger. In 2011 to 2012, she was a visiting researcher at Denmark Technical University, Photonics Department, where she worked toward spectrum-flexible cognitive optical networks and advanced modulation techniques for high-performance computing optical interconnects. From February 2013 to June 2018, Dr. Karinou worked as a Senior R&D Engineer in the Optical & Quantum Laboratory, at Huawei Technologies Duesseldorf GmbH, in the Huawei German Research Center in Munich, toward next generation high data-rate metro/access optical networks, optical interconnects for intra/inter data center networks, high-capacity coherent systems for long reach and quantum communications. In July 2018 she joined the Systems and Networking Group at Microsoft Research Ltd in Cambridge, UK, where she is working toward developing optical technologies for next generation cloud computing systems and networks. She has authored and co-authored more than 80 publications in the highest prestigious optical communications technology journals and conferences. She is/has served as Chair and TPC member in several (Optica, IEEE) conferences in the field of optical communications (OFC, CLEO, IPC, Photonics Society Summer Topical Meetings, OECC) and is currently serving as Associate Editor for the Journal of Lightwave Technology. Dr. Karinou has been engaged in several European research projects such as EU FP6 SECOQC, EU FP7 ICT-BONE, and EU FP7 CHRON projects.